ANTIOXIDANTS & REDOX SIGNALING
Volume 11, Number 8, 2009

DOI: 10.1089/ars.2008.2306

Original Research Communication

Overexpression of Mitochondrial Ferritin Sensitizes Cells to Oxidative Stress Via an Iron-Mediated Mechanism

Zhongbing Lu,[1] Guangjun Nie,[2] Yiye Li,[2] Shan Soe–lin,[3] Yi Tao,[1] Yuanlin Cao,[1] Zhiyong Zhang,[4] Nianqing Liu,[4] Prem Ponka,[3] and Baolu Zhao[1]

Abstract

Mitochondrial ferritin (MtFt) is a newly identified H-ferritin-like protein expressed only in mitochondria. Previous studies have shown that its overexpression markedly affects intracellular iron homeostasis and rescues defects caused by frataxin deficiency. To assess how MtFt exerts its function under oxidative stress conditions, MtFt overexpressing cells were treated with *tert*-butyl-hydroperoxide (tBHP), and the effects of MtFt expression on cell survival and iron homeostasis were examined. We found that MtFt expression was associated with decreased mitochondrial metabolic activity and reduced glutathione levels as well as a concomitant increase in reactive oxygen species levels and apoptosis. Moreover, mechanistic studies demonstrated that tBHP treatment led to a prolonged decrease in cytosolic ferritins levels in MtFt-expressing cells, while ferritin levels recovered to basal levels in control counterparts. tBHP treatment also resulted in elevated transferrin receptors, followed by more iron acquisition in MtFt expressing cells. The high molecular weight desferrioxamine, targeting to lysosomes, as well as the hydrophobic iron chelator salicylaldehyde isonicotinoyl hydrazone significantly attenuated tBHP-induced cell damage. In conclusion, the current study indicates that both the newly acquired iron from the extracellular environment and internal iron redistribution from ferritin degradation may be responsible for the increased sensitivity to oxidative stress in MtFt-expressing cells. *Antioxid. Redox Signal.* 11, 1791–1803.

Introduction

Ferritins are highly conserved ubiquitous iron-storage proteins that play a critical role in iron metabolism. Cytosolic ferritins consist of 24 subunits that form a spherical shell accommodating up to 4,500 iron atoms (10, 17, 43, 53). Nearly all of the cellular ferritins are found in the cytoplasm and the expression of ferritins is largely controlled post-transcriptionally by iron (10, 17, 43, 53). Cytosolic ferritin is composed of heavy (H) and light (L) subunits that have roughly 50% primary sequence identity. The H subunit has ferroxidase activity that is essential for the oxidation of incoming ferrous ions as ferric-oxohydrate phosphate, while the L subunit has a nucleation site that is involved in iron-core formation (10, 17, 43, 53). The cooperation of both subunits eventually leads to storage of iron as polymers of ferric-oxohydrate phosphate.

Ferritins are at the crossroads of iron and oxygen metabolism (52). A major function of ferritin is to limit Fe available to participate in the generation of oxygen free radicals. Numerous studies have already demonstrated that cytosolic ferritins provide the major protection against oxidative stress and the sensitivity of cells to oxidants is inversely correlated with ferritin protein levels (2, 13, 32, 53). Moreover, oxidative stress activates multiple pathways of ferritin regulation and both transcriptional and posttranscriptional mechanisms have been implicated in ferritin induction by oxidants (1, 53).

[1]State Key Laboratory of Brain and Recognition Laboratory, Institute of Biophysics, [2]Key Laboratory for Biomedical Effects of Nanomaterials and Nanosafety, National Center for Nanosciences and Technology of China and Institute of High Energy Physics, and [4]Sychrotron Radiation Laboratory, Institute of High Energy Physics, Chinese Academy of Sciences, Beijing, China.
[3]Lady Davis Institute for Medical Research, Sir Mortimer B. Davis Jewish General Hospital and Departments of Physiology and Medicine, McGill University, Montreal, Quebec, Canada.
Zhongbing Lu and Guangjun Nie contributed equally to this study.

Mitochondrial ferritin (MtFt) is a recently identified ferritin heavy chain-like protein (24). In both humans and mice, MtFt is encoded by an intronless gene, previously discovered as a pseudogene (24) and is expressed as a precursor protein that possesses a mitochondrial leader sequence and is targeted exclusively to mitochondria (7, 11, 24, 31). A recent study by Missirlis *et al.* showed that *Drosophila* expresses MtFt from an intron-containing gene and the protein has high similarity to mouse and human mitochondrial ferritins and is also preferentially expressed in testes (28). After the ferritin precursor is imported into the mitochondria, it is processed to an ~22 kDa mature protein in the mitochondrial matrix (7, 31), where it assembles into homopolymeric ferritin shells with ferroxidase activity (23). Under physiological conditions, MtFt is expressed at extremely low levels in most cells and tissues except the testes (11, 24, 47) where it is very highly expressed. The fact that the protein was also identified in heart, brain, spinal cord, kidney, and pancreatic islet of Langerhans, but not in liver and splenocytes, indicates that the major role of MtFt may be responsible for protecting mitochondria from iron-dependent oxidative damage in cells characterized by high metabolic activity and oxygen consumption, rather than for storing iron (47). Hepatocytes serve as depots for iron storage and have a large capacity to store excess iron, mainly in cytosolic ferritin. It is worth pointing out that the liver appears to represent a notable exception from the relationship between MtFt and high metabolic activity. Additionally, although MtFt is not normally present in erythroblasts, it is highly expressed in mitochondria of erythroblasts ("ringed sideroblasts") of patients with X-linked sideroblastic anemia (SA), as well as those with refractory anemia with ringed sideroblasts (6). It is well known that ringed sideroblasts are pathologic erythroid precursors containing excessive mitochondrial deposits of non-heme iron with a characteristic perinuclear distribution accounting for their ring appearance (3, 14, 26). Importantly, it has been shown that the iron in ringed sideroblasts is present within MtFt (6).

Mitochondria play a key role in iron metabolism (25, 29, 38, 46). Heme is synthesized in mitochondria, and iron–sulfur cluster (ISC) assembly occurs mainly, if not entirely, within these organelles (25, 29, 38, 46); hence, mitochondrial iron homeostasis must be tightly regulated. As these organelles are the major sites for the production of reactive oxygen species (ROS) that leak from the electron transfer chain as by-products (29, 33), excess iron, if in redox-active form, impairs the metabolic and respiratory activities of the mitochondria by catalyzing the Fenton reaction. Several human disorders characterized by mitochondrial iron overload have been linked with defects in mitochondrial iron transport and utilization (29).

Recent results from our laboratory (30, 31) as well as others (5, 7, 56) have shown that overexpression of MtFt leads to cellular iron redistribution whereby large amounts of iron are translocated to the mitochondria and stored within MtFt whose expression also rescued, at least partially, metabolic defects resulting from frataxin deficiency in both yeast and mammalian cells (5, 56). Although the regulation of MtFt expression and its function is not clearly known, it is likely that its presence plays an important role in both cellular iron and oxygen metabolism. To investigate how MtFt overexpression affects the response of cells to oxidative stress, we treated the well-characterized cell line H1299, which stably overexpresses mouse MtFt under the control of tetracycline, with tert-butyl hydroperoxide (tBHP). tBHP, among other organic hydroperoxides, such as cumene hydroperoxide, has been extensively employed as prototypic inducer of oxidative stress. It is thought that tBHP treatment leads to an oxidative stress that is more protracted compared with the effect of H_2O_2. H_2O_2 is metabolized more rapidly in cells than organic hydroperoxides (55). We show that MtFt induction leads to increased cellular ROS production and deleterious cell damage under oxidative stress conditions. This enhanced cell sensitivity to oxidative stress is associated with a prolonged decrease in cytosolic ferritin content, elevation of TfR levels, and increased iron uptake via the transferrin-TfR mediated iron acquisition pathway in MtFt-expressing cells. Our results indicate that MtFt expression-mediated mitochondrial iron accumulation increases cytosolic iron uptake and iron release from cytosolic ferritin. This increase in cytosolic iron content, which is likely redox-active, could contribute to the anemia and tissue damage seen during conditions of uncontrolled MtFt expression, such as X-linked SA, as well as refractory anemia with ringed sideroblasts.

Materials and Methods

Materials

Dulbecco's modified Eagle's medium (DMEM), fetal calf serum (FCS), 4-(2-hydroxyethyl)-1-piperazineethanesulfonic acid (HEPES), and 3-(4, 5-dimethylthiazol-2-yl)-2,5-diphenyltetrazolium-bromide (MTT) were purchased from Gibco BRL (Grand Island, NY). $^{59}FeCl_3$ was purchased from Perkin Elmer (Boston, MA). The iron chelator salicylaldehyde isonicotinoyl hydrazone (SIH) was synthesized as described by Ponka *et al.* (39). TRIzol® reagent and RT-PCR kit were purchased from Invitrogen (San Diego, CA). Anti-actin, Bcl-2, Bax, and hemagglutinin (HA) antibodies were purchased from Santa Cruz Biotechnology (Delaware, CA). Horseradish peroxidase-conjugated anti-rabbit, anti-mouse, and anti-horse immunoglobin G (IgG) were purchased from Sigma (Oakville, ON, Canada). Anti-transferrin receptor (TfR) antibody was purchased from Zymed (South San Francisco, CA) and anti-ferritin antibody was obtained from Dako (Carpinteria, CA). H-DFO was a generous gift from Biomedical Frontiers Inc. (Minneapolis, MN). All other reagents were purchased from Sigma unless otherwise specified.

Cell culture

The clone B9, stably overexpressing MtFt, was generated from the TA-H1299 cell line (non-small cell lung carcinoma) as described in a previous report (31). Cells were maintained in a medium consisting of DMEM supplemented with 10% (vol/vol) tetracycline-free fetal bovine serum (Clontech, Mississauga, ON, Canada), 2 m*M* glutamine, and 100 units/ml of penicillin and 0.1 ng/ml of streptomycin. MtFt expression was induced by removal of tetracycline (tet-off system).

Assessment of cell viability

The cells were cultured at a density of 2×10^4 cells/ml in 96-well plates 48 h before treatment. The culture medium was then replaced with fresh medium containing various concentrations of tBHP solution and incubated for 12 h to investigate the toxicity of tBHP. H-DFO or SIH was added 24 h

before tBHP treatment and maintained in the medium with/without tBHP. Cell viability was measured by the MTT colorimetric assay, which quantifies the mitochondrial activity of living cells. After treatment with tBHP for 24 h, the medium was removed and fresh medium containing 0.5 mg/ml MTT was added to each well, followed by incubation for 3 h at 37°C. Finally the medium containing MTT was removed, and DMSO was added to dissolve the formazan that forms from MTT. The absorbance at 595 nm was measured using a Bio-Rad 3350 microplate reader. Samples were measured in 8 replicates and each experiment was repeated at least three times. The values of the absorbencies were expressed as a percentage of control.

Detection of apoptosis by annexin V staining

Apoptosis induced by tBHP was measured by using an Annexin V-FITC kit according to the manufacturer's instructions (BioVision Inc., Palo Alto, CA). H1299 cells were plated at a density of 2×10^5 in 60 mm cell culture dishes and incubated overnight for cell attachment. After treatment with tBHP and/or H-DFO, cells were harvested and washed three times with cold 1×PBS, and resuspended in 500 μl of binding buffer. The cell suspension was incubated in a dark room for 15 min with 5 μl of Annexin V-FITC and 5 μl of propidium iodide (PI). Annexin V and PI emissions were detected in the FL1-H and FL2-H channels of a FACS Calibur flow cytometer (Becton Dickinson Immunocytometry System, San Jose, CA), using filters of 525 and 575 nm, respectively.

Measurement of intracellular ROS

The level of intracellular ROS was quantified by fluorescence with 2′, 7′-dichlorofluorescin diacetate (DCF-DA). After treatment, the cells were collected and washed three times with 1×PBS, then incubated with 5 μM DCF-DA for 45 min at 37°C in the dark. The cells were then washed three times with 1×PBS and resuspended in a buffer containing 130 mM NaCl, 5.4 mM KCl, 0.8 mM $MgCl_2$, 1.8 mM $CaCl_2$, 15 mM glucose, and 5 mM HEPES, pH 7.4. The relative levels of fluorescence were quantified by a spectrophotofluorometer (Hitachi F-4500, Tokyo, Japan, 485 nm excitation and 535 nm emission). The data were expressed as a percentage of the fluorescence relative to the fluorescence in the control cells.

Analysis of intracellular glutathione (GSH) and oxidized gGlutathione (GSSG)

To measure the amount of GSH and GSSG, we used a high performance liquid chromatography (HPLC) electrochemical system (ESA delivery system) equipped with a Supelcosil LC18 reversed-phase column (250×4.6 mm; 5 μm particle size, Supelco Inc., Bellefonte, PA) and Coularray electrochemical detector (ESA Inc., Chelmsford, MA). As described previously (57), the mobile phase consisted of 50 mM sodium dihydrogen phosphate and 2% acetonitrile (pH = 2.7). The analysis was carried out at a column temperature of 25°C with a 20 μl sample injection and a flow rate of 1.0 ml/min. The potential of channels 1, 2, 3, and 4 were set to 400, 600, 800, and 1,000 mV, respectively. The peak area was used to calculate the concentration. Calibration was achieved by simultaneously measuring standard GSH and GSSG dissolved in 10 mM HCl. After treatment, $\sim10^6$ cells were collected with two PBS washes, and the cells were homogenized with 100 μl aqueous trichloroacetic acid (5%, wt/vol) to precipitate proteins. After centrifugation at 12,000 g for 10 min at 4°C, the supernatant was diluted with 10 mM HCl and the amounts of GSH and GSSG were measured with HPLC–ECD. The chromatograms were analyzed and the amounts of GSH and GSSG were calculated with Coularraywin software (ESA Inc., Bedford, MA).

Measurement of mitochondrial membrane potential

The mitochondrial membrane potential was measured by the incorporation of the cationic fluorescent dye rhodamine 123. After 24 h incubation in normal medium with or without treatment, the cells were changed to serum-free medium containing 10 μM rhodamine 123 and incubated for 15 min at 37°C. The cells were then collected and the fluorescence intensity was analyzed within 15 min by a spectrophotofluorometer (Hitachi F-4500, 490 nm excitation and 515 nm emission).

Western blot analysis

To detect the variations in protein expression, control and treated cells were lysed in lysis buffer (50 mM Tris-HCl, 150 mM NaCl, 0.02% (wt/vol) NaN_3, 100 μg/ml PMSF, 1 μg/ml aprotinin, 1 μg/ml pepstatin A, 2 μg/ml leupeptin, and 1% (vol/vol) Triton-X 100) on ice for 30 min and then centrifuged at 12,000 g for 20 min. The supernatant was used for SDS-PAGE and protein content was estimated by a BCA kit (Pierce, Rockford, IL). 40 μg protein equivalents of each sample were loaded in SDS-PAGE. Proteins were separated on gels and transferred to a nitrocellulose membrane. Blots were blocked in a blocking buffer containing 5% nonfat milk, 0.1% Tween 20 in 0.01 M TBS, and incubated with primary antibody overnight with constant agitation at 4°C. The membrane was then incubated with the secondary antibody for 1 h at room temperature with constant agitation, then washed and reacted with the supersignal chemiluminescent substrate (Pierce), and exposed to Kodak-XAR film. The film was digitized and analyzed by NIH imaging software.

RT–PCR assay

Total RNA was extracted from cells with TRIzol® reagent (Invitrogen). 2 μg of total RNA was reverse transcribed into cDNA using the SuperScript First-Strand Synthesis System (Invitrogen). The primers were designed according to GenBank sequences. The PCR reaction solution was performed according to the following parameters: 95°C 45 sec, annealing temperature 30–60 sec, 72°C 45 sec, 30 cycles with TaKaRa Ex Taq™ Hot Start Version (Takara, Otsu, Shiga, Japan) in a MJ Research PTC-200 Peltier Thermor Cycler (Ramsey, MN). 10 μl of the PCR reaction was electrophoresed on a 2% agarose gel. The primers used for the PCR reaction were as follows: TfR Sense: 5′-AGCACAGACTTCACCAGCAC-3′, Antisense: 5′-GTCCCCAGATGAGCATGTCC-3′ (506bp).

Iron uptake

Human apo-transferrin was labeled with ^{59}Fe, as described previously (40). 3×10^6 cells were seeded with or without tetracycline, cultured for 48 h, and then treated with tBHP (at initial concentrations of 30, 50, or 100 μM) for 3 h, followed

by incubation for 3 h with 1 μM ^{59}Fe-transferrin at 37°C. The cells were then washed three times with ice-cold PBS and the radioactivity in the cell pellet and culture medium was measured by a gamma counter (Cobra II auto-gamma, Packard, Ramsey, MN).

Ferritin ELISA

Cellular proteins were extracted with 150 mM NaCl, 10 mM EDTA, 40 mM Tris (pH7.4), 1% Triton X-100, and a protease inhibitor cocktail (Roche, Palo Alto, CA). Total protein concentration was determined using the BCA reagent (Pierce). B9 cells were induced to express MtFt by removal of tet from the culture medium for 24 h, followed by treatment with or without H-DFO and tBHP. Ferritin levels from B9 cell extracts were determined by ELISA (Laguna Scientific, Laguna, CA) according to the manufacturer's instructions.

Assay of lysosomal stability

The lysosomal stability in cells was measured using the acridine orange (AO) relocation method according to Kurz *et al*. (22). AO is a metachromatic fluorophore (red at high concentrations and green at low concentrations) and a lysosomotropic base (p$Ka = 10.3$). When cells are preloaded with AO, the fluorescent dye will be mainly retained in its charged form by proton trapping preferentially inside acidic secondary lysosomes (pH 4–5). The cells then show intense granular red fluorescence with faint green cytosol and nuclei. The red fluorescence indicates aggregation of acidified AO in the lysosomes, whereas green fluorescence accounts for lower concentrations of AO in the cytosol and nuclei, hence an increase of the green fluorescence will be indicative for AO released from the lysosomal compartment and early lysosomal rupture due to oxidative stress. Briefly, B9 cells were incubated with or without SIH for 12 h, then preloaded with AO (5 μg/ml) for 15 min, followed by treatment with tBHP at an initial concentration of 90 μM for 3 h, or left untreated. After two washes with PBS, the fluorescence of the samples was then measured by flow cytometry to monitor early lysosomal rupture and the resulting AO relocation. Green (FL1 channel) fluorescence was recorded in logarithmic scale, using Cell Lab Quanta™ SC flow cytometer (Beckman Coulter, Fullerton, CA) equipped with a 488 nm exciting argon laser and appropriate barrier filters.

Statistical analysis

All experiments were performed in triplicate unless otherwise indicated. Results are representative of three independent experiments. Error bars represent standard deviations. A probability level of 5% ($p < 0.05$) was considered significant.

Results

MtFt expression increases cell death following tBHP treatment

MtFt is a novel H-ferritin-like protein which is exclusively targeted to mitochondria. To examine whether the induction of MtFt expression affected cell resistance to oxidative stress, we treated B9 cells with tBHP, with or without the presence of tetracycline (MtFt suppressed or induced cells, respectively). tBHP treatment caused a concentration-dependent induction of cell death, which occurred at initial concentrations as low as 40 μM (Fig. 1A). Although concentrations of tBHP (40–60 μM) decrease cell viability of both MtFt suppressed and induced cells, these effects are more pronounced in MtFt induced cells (Fig. 1A). In the presence of an initial concentration of 70 μM tBHP, the cell viability decreased to 10% and there are no statistical differences between MtFt suppressed and induced cells, indicating that higher concentration of tBHP may diminish the effect of MtFt expression.

To confirm this unexpected observation, which is contrary to our original prediction that MtFt expression may prevent cell damage induced by oxidative stress as observed in cytosolic ferritin studies (2, 13, 20), we quantified the actual extent of apoptosis in tBHP treated B9 cells in the presence or absence of tet using annexin and PI staining, followed by cell flow cytometry measurement. The results confirmed that the protein expression itself caused increased cell sensitivity to tBHP treatment and led to increased cell death. As shown in Fig. 2B, exposure of B9 cells to an initial concentration of 40 μM of tBHP increased the fraction of apoptotic Annexin positive cells from $2.8 \pm 1.5\%$ to $14.4 \pm 2.5\%$ ($p < 0.01$). The induction of MtFt expression by removal of tet for 2 days, substantially elevated the fraction of apoptotic annexin-positive cells from $14.4 \pm 2.5\%$ to $21.8 \pm 3.4\%$ ($p < 0.01$).

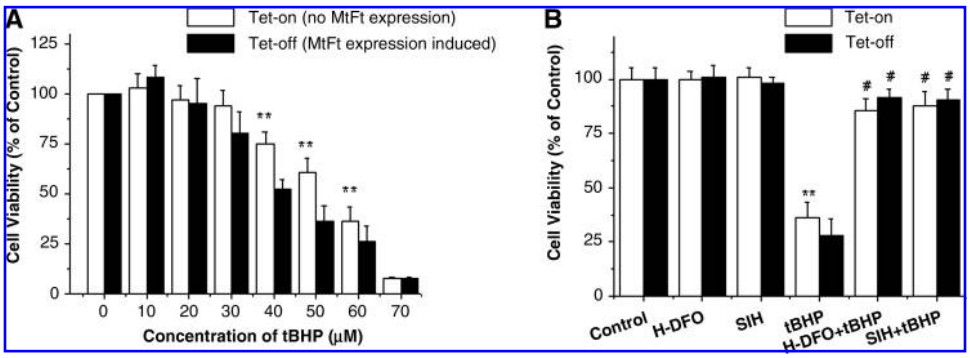

FIG. 1. MtFt expression increases cell death induced by tBHP treatment. (**A**) B9 cells stably transfected with mouse MtFt, were cultured with tet (tet-on) or without tet (tet-off) for 48 h, followed by tBHP treatment for 12 h. The cell viability was measured by MTT assay. (**B**) H-DFO or SIH treatment significantly prevents the loss of cell viability. The same cells as described in (**A**) were preloaded with 100 μM of H-DFO or SIH 24 h before tBHP treatment (60 μM). Data are expressed as percentage of cell viability compared to untreated control cells ± SEM, $n = 8$. $^{**}p < 0.01$ MtFt induced groups *vs*. MtFt uninduced groups, respectively; $\#p < 0.05$ the cells pretreated with H-DFO or SIH *vs*. the cells without H-DFO or SIH pretreatment, respectively.

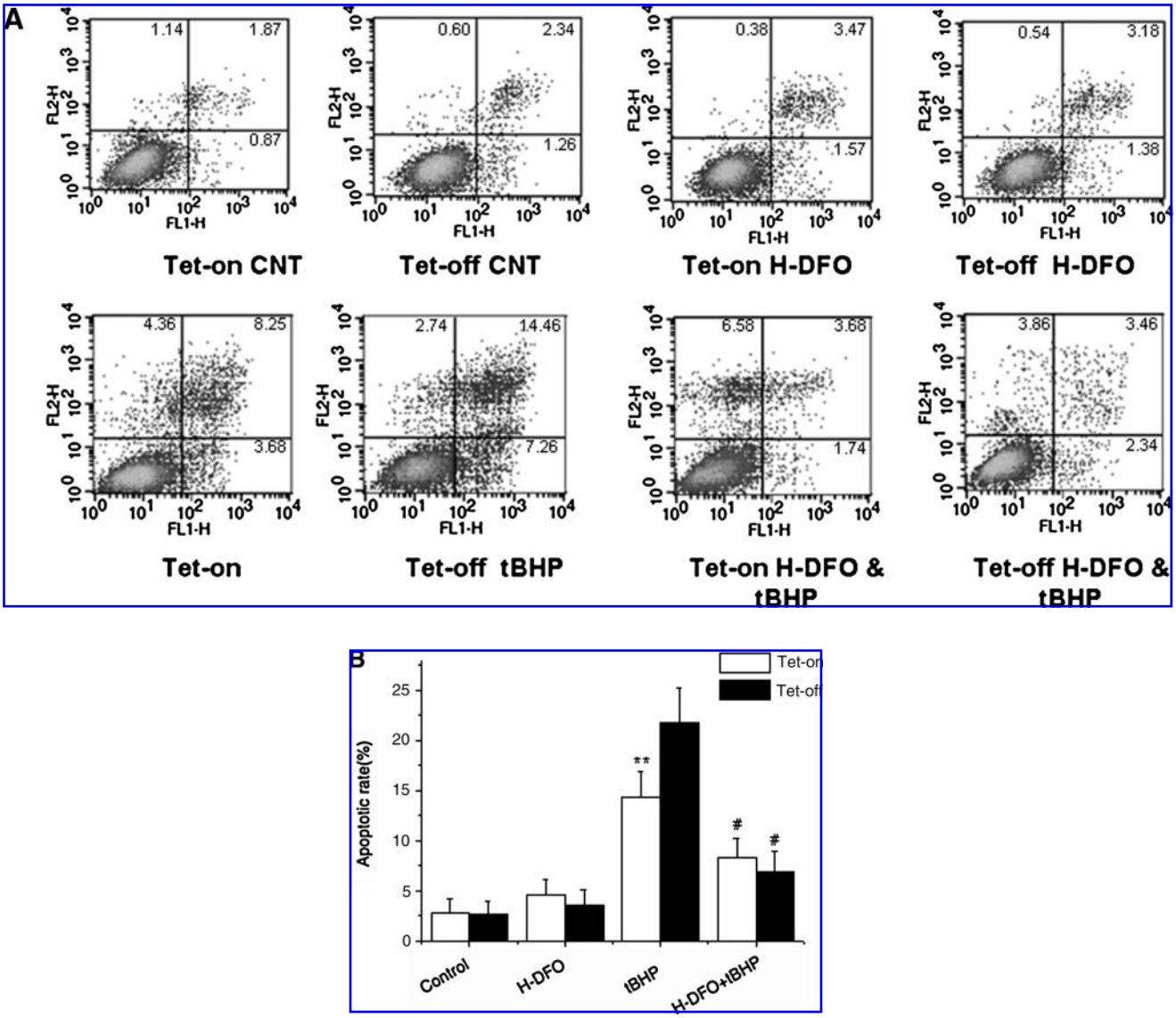

FIG. 2. MtFt expression sensitizes for tBHP-induced apoptosis. (**A**) Representative flow cytometry histographs depict the differential effects of tBHP treatment on MtFt induced and uninduced cells. Cells were cultured with or without tet for 48 h followed by incubation with or without 40 μM t-BHP for 12 h. As indicated, 100 μM of H-DFO was added 24 h before tBHP treatment and allowed to remain in the medium. CNT, B9 cells without treatment; H-DFO, cells treated with 100 μM H-DFO; tBHP, cells treated with 40 μM tBHP. (**B**) Statistical analysis of flow cytometry results. Data were expressed as mean ± SEM, $n = 3$. $^{**}p < 0.01$ tet-on cells *vs*. tet-off cells under the treatment of tBHP; $\#p < 0.05$ tet-on and tet-off cells without H-DFO treatment *vs*. H-DFO pretreatment, respectively.

Iron chelators attenuated tBHP- induced cell death

We have demonstrated previously that MtFt expression dramatically changed intracellular iron metabolism (31). In support of the hypothesis that iron plays a pivotal role in tBHP-induced cell death, we consistently observed that two well-established iron chelators, high molecular weight desferrioxamine (H-DFO, 75 kD) (16, 36) and salicylaldehyde isonicotinoyl hydrazone (SIH) (39) significantly protected cells from damage induced by oxidative stress. Pretreatment with either H-DFO or SIH (Fig. 1B) markedly attenuated tBHP-induced cell death in both induced and uninduced cells. Pretreatment with 100 μM H-DFO increased cell viability from $\sim 37 \pm 7.0\%$ to $88 \pm 5.4\%$ ($p < 0.05$) and $28 \pm 7.3\%$ to $94 \pm 3.8\%$ ($p < 0.05$) in MtFt uninduced and induced cells, respectively, following exposure to an initial concentration of 60 μM tBHP (Fig. 1B). SIH pretreatment has the similar effects. H-DFO pretreatment also significantly reduced tBHP-induced apoptosis (Fig. 2). Figure 2B shows the quantitative results of H-DFO pretreatment attenuation of apoptosis (the frequency of apoptotic events dropped from $21.8 \pm 3.4\%$ to $6.9 \pm 2.1\%$ in MtFt induced cells ($p < 0.05$) and from $14.4 \pm 2.5\%$ to $8.3 \pm 1.9\%$ in uninduced cells ($p < 0.05$), respectively). Previous studies have shown that cytosolic ferritins are mainly degraded in lysosomes and iron can be recycled through this degradation pathway (41). These findings, combined with the observation that H-DFO targets exclusively to lysosomes

(22, 35–37), imply that iron released from ferritins and other iron containing proteins could be chelated by H-DFO, which blocks the transport of iron to cytosolic or mitochondrial compartments.

MtFt expression significantly disrupts cellular redox homeostasis under oxidative stress conditions; iron chelators can prevent the disturbance

To directly monitor the cytotoxicity of tBHP, we measured the intracellular levels of ROS, which are thought to directly lead to cell damage in both induced and uninduced cells. Figure 3A showed that an initial concentration of 50 μM of tBHP treatment for 6 h led to a 75% increase in intracellular ROS. Interestingly, MtFt expression resulted in a further increase in ROS levels from 175% of basal level in the uninduced cells to 225% of basal level in the induced cells. Moreover, H-DFO pretreatment decreased ROS to basal levels in both induced and uninduced cells (Fig. 3A); H-DFO itself did not affect cellular ROS levels.

The mitochondrial membrane potential reflects the integrated metabolic function of mitochondria. As shown in Fig. 3B, tBHP decreased the mitochondrial membrane potential as demonstrated by the decrease in rhodamine 123 fluorescence intensity. Importantly, MtFt expression further decreased the mitochondrial membrane potential (Fig. 3B). Moreover, H-DFO pretreatment largely prevented mitochondrial membrane potential loss induced by tBHP assault (Fig. 3B).

Glutathione (GSH) is a cellular antioxidant that is known to prevent oxidative stress-induced cell damage (9). GSH levels directly reflect cellular redox status (9). Figure 3C shows that tBHP treatment greatly decreased cellular levels of glutathione and that the decrease in GSH levels was more prominent in MtFt induced cells. H-DFO pretreatment efficiently restored the decrease in GSH levels in both MtFt induced and uninduced cells (Fig. 3C). Moreover, the intracellular levels of GSSG (the oxidized form of glutathione) were dramatically increased in tBHP treated cells, especially in MtFt induced cells (Fig. 3D). Additionally, H-DFO treatment restored GSSG levels to baseline (Fig. 3D).

Taken together, these results are consistent with the observation that MtFt expression increases cell death under tBHP treatment. MtFt-induced cells generate more ROS and contain less GSH, and have a lower mitochondrial membrane potential. Based on these results, we speculate that MtFt expression significantly increases intracellular ROS levels in the cells following tBHP treatment.

tBHP treatment lowers the Bcl-2/Bax ratio

Bcl-2 and Bax are anti-apoptotic and pro-apoptotic proteins, respectively. The Bcl–2/Bax ratio has been widely used to monitor apoptosis (27, 42). To address whether Bcl-2 and Bax levels correlate with the apoptosis that occurred after tBHP treatment, the Bcl–2/Bax ratio was quantified from total cell extracts. When B9 cells were incubated with an initial concentration of 50 μM tBHP, the levels of Bcl-2 decreased slightly after 12 h of culture, whereas a marked increase in Bax was observed following the treatment (Fig. 4A). These results are consistent with measurements by flow cytometry of apoptosis (Fig. 2). Therefore, the decrease in the Bcl–2/Bax ratio (Fig. 4B) may be responsible for the apoptosis observed following tBHP treatment. MtFt expression slightly, but not significantly, correlated with a decrease in protein expression. Additionally, H-DFO pretreatment restored the expression of Bcl-2 and Bax proteins to basal levels (Fig. 4).

tBHP treatment and MtFt expression alter cellular iron homeostasis

Our previous studies showed that MtFt expression induced cytosolic iron deficiency as demonstrated by increased TfR levels, decreased cytosolic ferritin levels, and stimulated iron

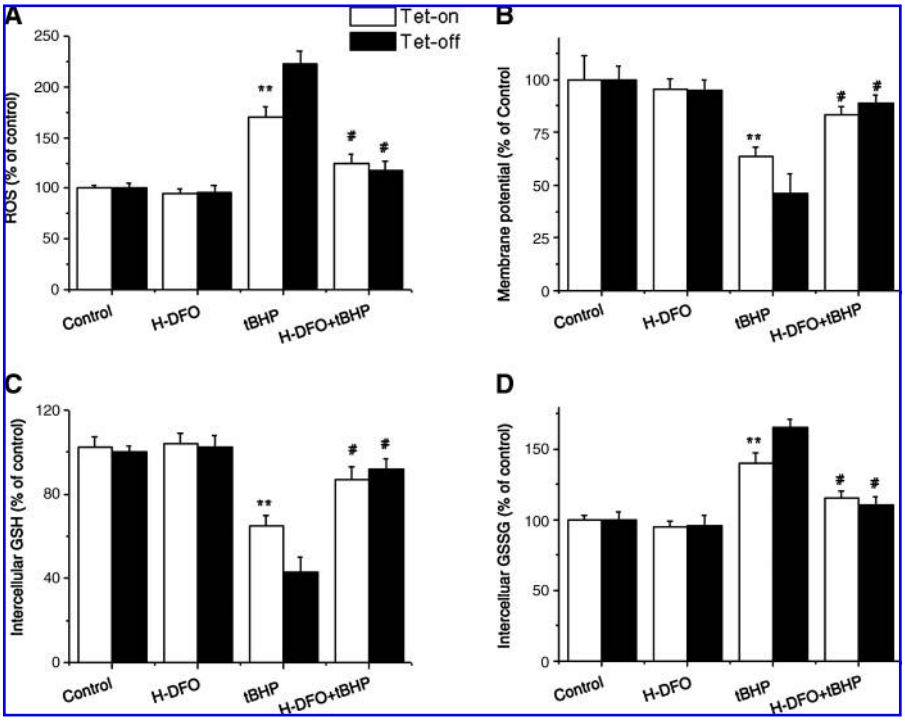

FIG. 3. MtFt expression exacerbates cell oxidative stress induced by tBHP. (**A**) MtFt expression leads to more intracellular ROS production under tBHP treatment (50 μM) measured by DCFDA fluorescence; (**B**) MtFt expression results in further loss of mitochondrial membrane potential following tBHP treatment (50 μM). (**C**) and (**D**): MtFt expression resulted in decreased GSH (**C**) and increased GSSG (**D**) content following tBHP treatment (50 μM). Data were expressed as percentage of control groups $\pm$ SEM, $n = 3$ (**$p < 0.01$ tet-on cells *vs.* tet-off cells; #$p < 0.05$ tet-on and tet-off cells without H-DFO treatment *vs.* H-DFO pretreatment, respectively).

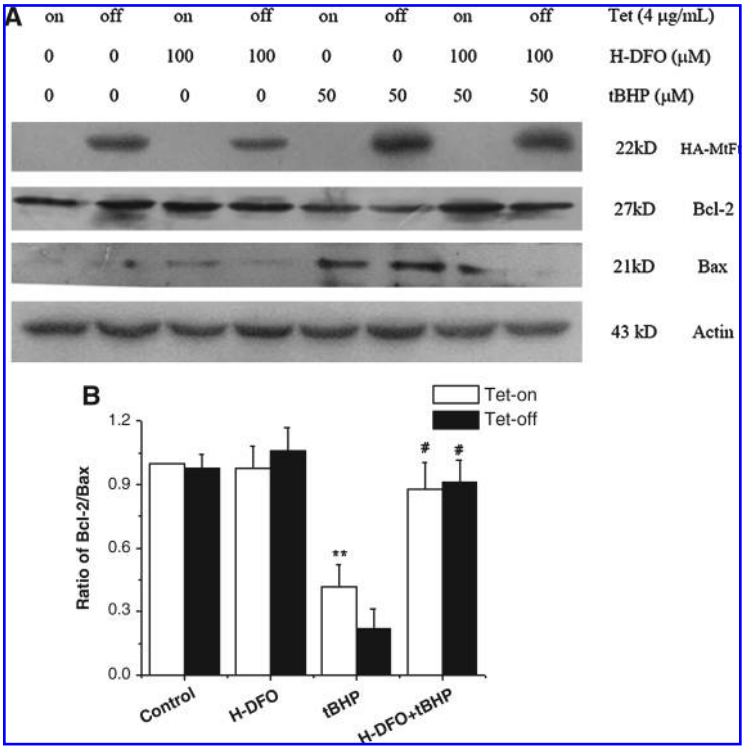

FIG. 4. tBHP treatment significantly reduces Bcl-2/Bax ratio and MtFt expression further lowers the Bcl-2/Bax ratio. (**A**) Aliquots of total cell extracts were analyzed by Western blot using anti-Bcl-2, Bax, β-actin, and HA antibodies. (**B**) Ratio between band intensities of Bcl-2 *vs*. Bax corresponding to the cells with different treatments (mean $\pm$ SEM, $n = 3$, $^{**}p < 0.01$ tet-on cells *vs*. tet-off cells following tBHP treatment, $\#p < 0.05$ tet-on and tet-off cells without H-DFO treatment *vs*. H-DFO pretreatment, respectively).

uptake from transferrin (31). In the current study, we further investigated the changes to intracellular iron metabolism caused by induction of MtFt expression and oxidative stress by tBHP treatment. First, our results showed that both tBHP treatment and MtFt expression stimulated TfR protein expression (Fig. 5A and C). Consistent with our previous observations, MtFt expression increased TfR expression ($\sim$1.8-fold compared to MtFt uninduced cells). A dramatic elevation of TfR levels occurred following 50 μM of tBHP treatment in both MtFt uninduced cells ($\sim$2.2-fold) and induced cells ($\sim$2.8-fold), as compared to untreated cells (Fig. 5A and C). MtFt expression and tBHP treatment were found to exert a synergetic effect on TfR expression, resulting in a 1.8-fold to 2.8-fold increase in basal TfR content (Fig. 5A, lane 6). As expected, 100 μM H-DFO had the most significant effect on TfR expression (2.7- and 4.9-fold increase in MtFt uninduced cells and induced cells, respectively) (Fig. 5A and C).

Further studies exploiting semiquantitative RT–PCR demonstrated that tBHP treatment and MtFt expression significantly increased TfR mRNA (Fig. 5B and D). The changes in TfR transcript levels occur most likely via IRE–IRP mediated stabilization of TfR mRNA following iron deficiency and activation of IRP1 by oxidants (4, 43).

Ferritin, a cytoprotective protein whose genes are responsive to oxidative stress, serves as the major iron-binding protein in nonhematopoietic tissues and limits the catalytic availability of iron for participation in oxygen radical generation (54). Figure 6A shows that steady-state levels of cytosolic ferritins were significantly reduced after induction of MtFt. As expected, 100 μM H-DFO treatment caused the most profound decrease in ferritin levels (Fig. 6A). Interestingly, an initial concentration of 50 μM tBHP treatment for 12 h had little effect on steady-state level of ferritins in both MtFt induced and uninduced cells in comparison with their untreated counterparts. Previous studies have shown that hydrogen peroxide treatment inhibits ferritin synthesis for 8 h and leads to a significant reduction of ferritin content (4). To further investigate the effect of a sublethal concentration of tBHP (30 μM) treatment on ferritin expression, we measured ferritin content over 24 h to observe the dynamic change of the proteins. Figure 6B shows a time-dependent decrease in cytosolic ferritin protein levels in both MtFt induced and uninduced cells following 7–8 h of tBHP treatment. This observation is consistent with the results from hydrogen peroxide treatment (4). Interestingly, ferritin protein levels began to recover and reached basal levels in MtFt uninduced cells ($\sim$43 ng/mg protein) 24 h after the treatments, but MtFt induced cells were less able to recover baseline ferritin levels (24 ng/mg protein) (Fig. 6B), indicating that the induction of MtFt resulted in a prolonged decrease in cytosolic ferritin levels. Since cytosolic ferritin exerts significant cytoprotective effects under oxidative stress conditions, the difference in cytosolic ferritin expression in MtFt-induced and uninduced cells could largely explain why MtFt-induced cells are more sensitive to oxidative stress catalyzed by redox reactive iron. Moreover, iron released from cytosolic ferritin is most likely mobilized to other cellular compartments, which could transiently participate in iron-mediated Fenton reactions, consequently, lead to severe cell damage. H-DFO targets to the lysosomes (36, 37) where cytosolic ferritin degradation mainly occurs (41), and the blocked release of iron from lysosomes by H-DFO was found to greatly attenuate tBHP induced cell damage (Fig. 1B).

MtFt expression leads to elevated uptake of ^{59}Fe-transferrin under tBHP treatment

To examine whether stimulation of TfR expression by tBHP is associated with increased in iron uptake, we analyzed total iron uptake following increasing concentrations of tBHP

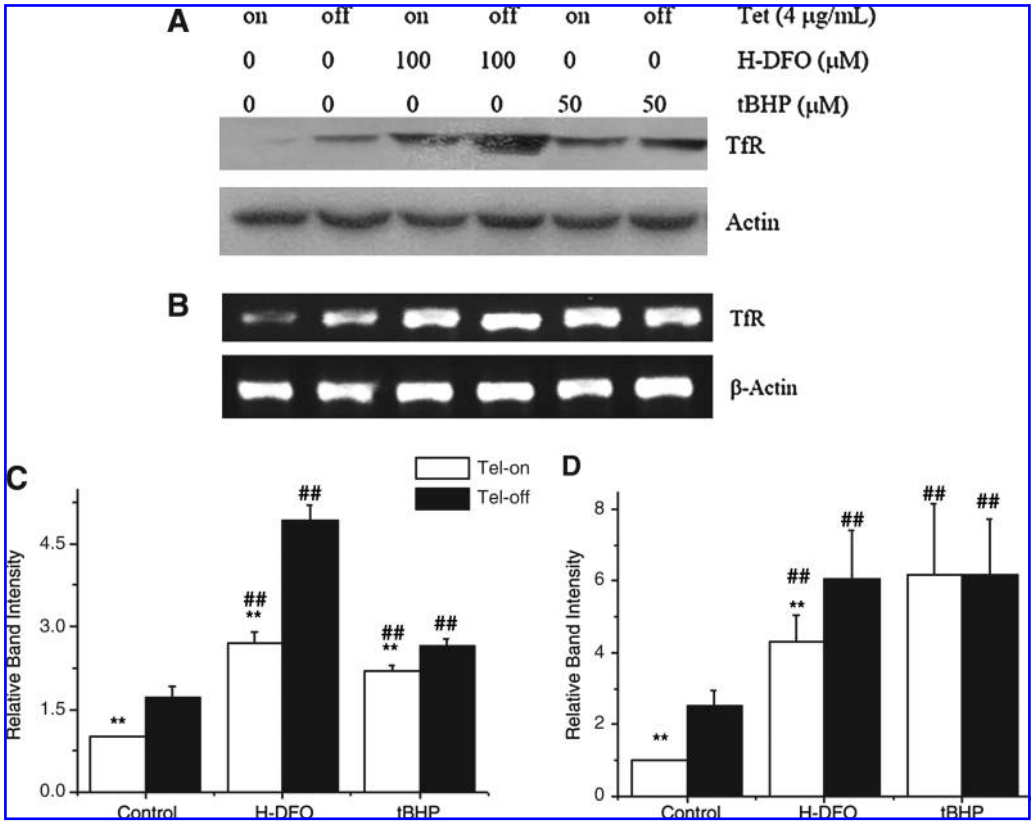

FIG. 5. MtFt expression and tBHP treatment up-regulate TfR mRNA level and protein expression. (**A**) Western blot analysis of TfR protein expression. (**B**) RT-PCR measurement of TfR mRNA level. (**C**) Relative analysis of TfR and β-actin protein expression. (**D**) Semi-quantitative analysis of TfR and β-actin mRNA level. The data were presented as mean $\pm$ SEM, $n = 3$, $^{**}p < 0.01$ compared with tet-on cells. ## $p < 0.01$ tet-on and tet-off cells following tBHP or H-DFO treatment *vs*. control cells, respectively.

(initial concentrations of 0–100 μM of tBHP). Our results showed that increased TfR levels were associated with increased iron acquisition as evidenced by the 30–45% increase in iron uptake seen in MtFt induced cells compared to their uninduced counterparts for all the tBHP concentrations (Fig. 7). However, the increase in TfR expression following tBHP treatment did not lead to a proportional increase in iron uptake in comparison with tBHP-untreated cells; rather all tBHP-treated samples had less iron acquired via TfR-transferrin, although they had higher amounts of TfR (Fig. 7). This observation may implicate targets, other than TfR, in the TfR–transferrin iron acquisition pathway that could be suppressed by oxidants. Overall, tBHP treatment results in reduced iron uptake compared to tBHP untreated cells; thus, a decrease in iron acquisition may be helpful for cell resistance against oxidative stress.

tBHP treatment and MtFt expression alter lysosome stability

The intensity of intracellular green fluorescence of AO was used to measure the stability of lysosomes. As shown in Fig. 7B, an initial concentration of 90 μM tBHP treatment significantly elevated intracellular green fluorescence compared with the control counterparts, while SIH treatment and MtFt expression only slightly increased green fluorescence in the cells. The tet-off cells showed more intracellular green fluorescence compared to tet-on cells, and iron chelator pretreatment led to a dramatic decrease in green fluorescence (Fig 7B). It should be noted that the observed differences (among tet-on and tet-off cells either pretreated with SIH or not) are seen only in context with exposure to tBHP. Exposure to a highly cytotoxic regimen of tBHP may stimulate a rapidly developing necrotic mode of cell death, featured by an early cell lysis, lysosomal rupture, and rapid cellular disintegration, although trypan blue staining experiments showed that this type of cell death was negligible. Taken together, our results indicate that MtFt expression exacerbates the lysosomal destabilization induced by tBHP via the increase of lysosomal redox-active iron.

Discussion

Iron is a precious metal for organisms and is involved in a broad spectrum of essential biological functions (17, 43). However, some aspects of iron chemistry diminish this metal's appeal for biological systems. Unless bound to specific ligands, at pH 7.4 and under physiological oxygen tension, iron would exist only in the form of virtually insoluble ferric hydroxide. Moreover, iron's catalytic action in one-electron redox reactions can play an important role in the formation of toxic free radicals that ultimately cause oxidative damage to vital cell structures (1, 12). Therefore, organisms are equipped with specific proteins designed for this metal's acquisition, transport, and storage in a soluble nontoxic form.

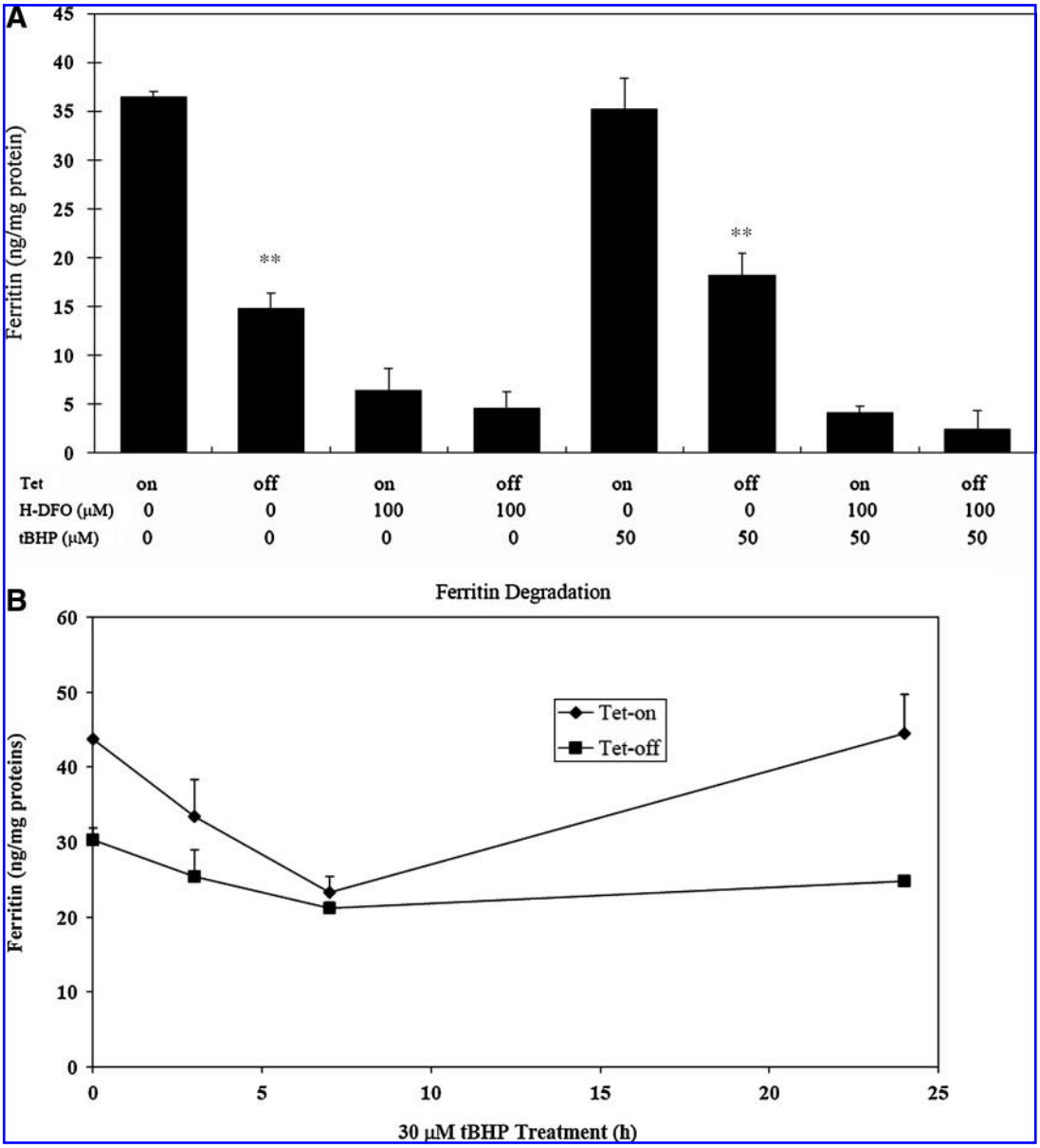

FIG. 6. MtFt expression altered intercellular Ferritin level. (**A**) MtFt-mediated decrease in ferritin is further augmented by H-DFO treatment, but not by t-BHP treatment after 12 h treatment. (**B**) Ferritin degradation time course following 30 μM tBHP treatment. Data express mean ± SEM, $n = 3$, $^{**}p < 0.01$ tet-on cells *vs.* tet-off cells.

Under normal circumstances, MtFt is expressed mainly in testes (11). While MtFt is undetectable in normal erythroid cells, the ringed sideroblasts of SA patients have been shown to contain a large amount of MtFt (6, 51). Mitochondria play a key role in cellular iron metabolism, iron–sulfur cluster synthesis, and promotion of apoptosis under pathological conditions, such as oxidative stress. Mitochondrial iron levels must be well regulated, as an inadequate supply of iron would impair the metabolic and respiratory activities of the organelle, while excess iron in mitochondria would promote the generation of harmful ROS, which are generated during mitochondrial electron transport.

Although the physiological function of MtFt is still elusive, recent results from our laboratory (30, 31) and others (7) showed that overexpression of MtFt leads to a rapid and efficient redistribution of iron from various sources in the cytosol to mitochondria, and its sequestration in a form unavailable for metabolic use. Since MtFt expression prevented, at least in part, oxidative stress-induced damage of frataxin-defective yeast and HeLa cells (5, 56), we speculated that the expression of MtFt may abrogate the toxic effects caused by oxidative stress in vitro. To assess how MtFt overexpression affects the response of cells to oxidative stress and to elucidate the role of MtFt expression in cells subjected to oxidative stress, we took advantage of a well- established cell model, in which MtFt can be overexpressed in a regulated manner.

Unexpectedly, we observed that MtFt expression increased cell damage caused by oxidative stress via an iron-mediated mechanism. Our results have shown that, in fact, MtFt expression potentiates tBHP-induced cell damage in B9 cells.

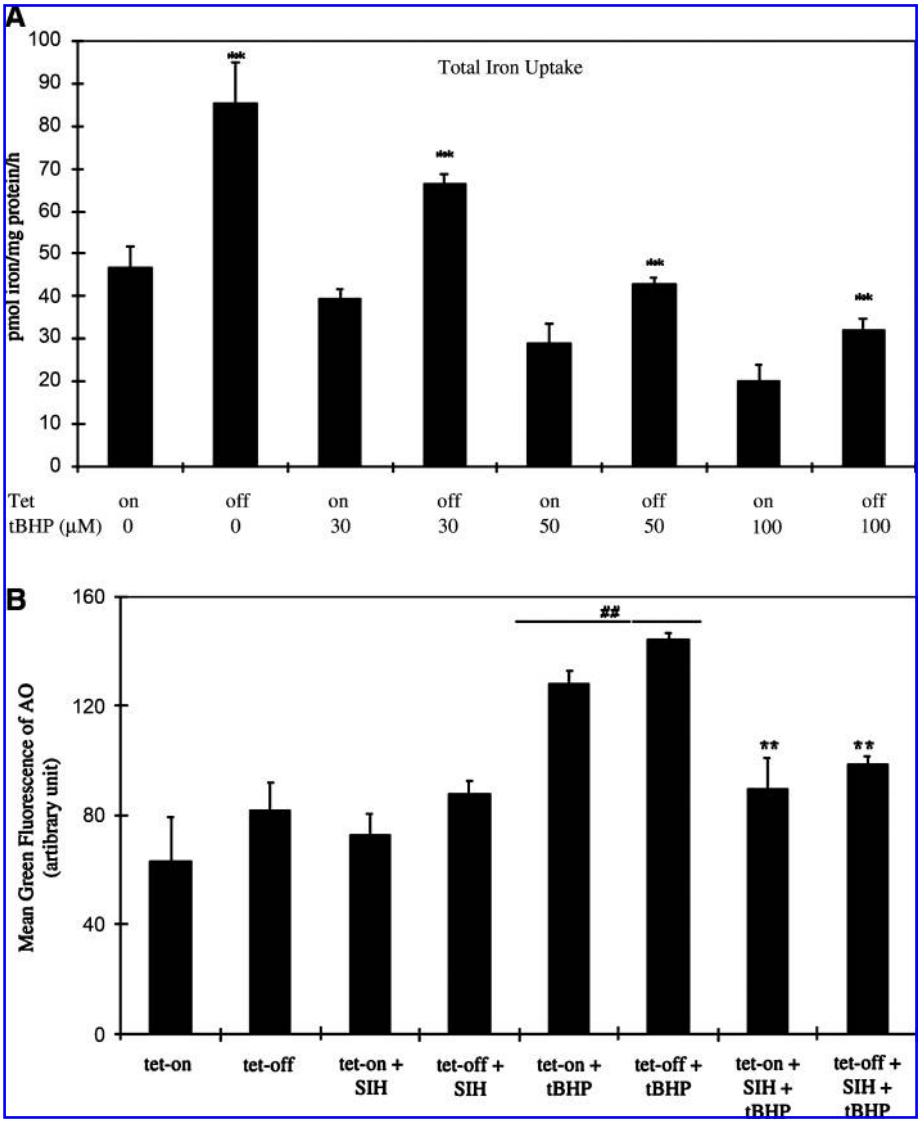

FIG. 7. Overexpression of MtFt enhances ^{59}Fe uptake from ^{59}Fe$_2$-transferrin and decreases lysosome stability following tBHP treatment. (**A**) B9 cells were grown for 48 h without or with tet, then treated with tBHP for 3 h, followed by incubation with 1 μM ^{59}Fe-transferrin for 1 h; after three washes with PBS, the cells' radioactivity was measured. (**B**) B9 cells were grown for 48 h without or with tet, followed by treatment with or without SIH for 12 h. The cells were then preloaded with AO (5 μg/ml) for 15 min, followed by treatment with or without 90 μM tBHP for 3 h. After two washes with PBS, green fluorescence was measured by FACS. Data shown are the mean $\pm$ SEM of triplicate determinations from a representative experiment of four repeats. $^{**}p < 0.01$ compared with tet-on cells under different tBHP treatment, respectively. $^{\#\#}p < 0.01$ compared with tet-on cells under different tBHP treatment.

This was demonstrated by decreased mitochondrial metabolic activity and membrane potential, reduced glutathione levels, and a concomitant increase in ROS production and apoptosis. To determine the involvement of iron in mediating cell damage under oxidative stress conditions, we investigated the relationship between oxidative stress damage and changes in cellular iron homeostasis caused by MtFt expression and tBHP treatment. We observed a dramatic increase in iron uptake via the transferrin–TfR pathway and a decrease in cytosolic ferritin in MtFt-expressing cells after tBHP treatment. More importantly, we also observed that lysosomes of MtFt-overexpressing cells are less stable as compared to their counterparts (Fig. 7B). This observation may indicate that iron-rich mitochondria (MtFt-overexpressing cells) are degraded intralysosomally, and the degradation of these mitochondria increases lysosomal redox-active iron and makes these organelles more vulnerable to oxidative stress due to enhanced formation of hydroxyl radicals that peroxidize and destabilize lysosomal membranes. This mechanism may account for, in part, the findings that release of iron inside lysosomes apparently renders MtFt-overexpressing cells more sensitive to oxidative stress; consequently, more severe apoptosis occurred in these cells. Previous studies have shown that quinone naphthzarine induced-oxidative stress causes relocation of the lysosomal enzymes, such as cathepsin D, which ensured apoptosis in neonatal cardiomyocytes (45); and the relocation of cathepsin D from lysosomes precedes mitochondrial membrane potential decrease and cytochrome c release from mitochondria during apoptosis (44). Therefore, we propose that increased levels of redox-active iron in the cytosol and/or mitochondria could originate from the extracellular environment (acquired via transferrin–TfR). Moreover, iron released in lysosomes from autophagocytosed cytosolic proteins, such as ferritin and perhaps other iron-containing molecules, may also be responsible for the deleterious effects of MtFt expression under oxidative stress conditions.

Elevated iron uptake via the transferrin-TfR pathway has been implicated in the cell damage caused by oxidative stress (21). As was confirmed in the current study (Fig. 6), this increased iron uptake from extracellular sources is, at least in part, responsible for the more severe cell damage observed in MtFt induced cells. H-ferritin has been found to significantly protect cells against oxidative stress induced by a variety of

sources (13, 32, 52). A marked induction of H-ferritin in HeLa cells attenuated cell damage in a manner which was dependent on its expression (8). Therefore, it appears that cell survival is closely dependent on the cellular level of ferritin. This hypothesis is also confirmed by our current study, as a profound decrease in cytosolic ferritin correlates with an increase in apoptosis in MtFt induced cells (Figs. 1, 2, and 6B). Oxidants can induce ferritin transcription by directly targeting conserved antioxidant-responsive elements of ferritin genes (54), but can also inhibit ferritin translation by mobilizing iron from the 4Fe–4S cubane of IRP1 (34). Our results are congruent with a recent study on the dynamic modulation of ferritin function and expression by oxidants (54). Ferritin translation was transiently inhibited by hydrogen peroxide treatment, followed by a sustained increase in ferritin transcription induced by oxidative stress.

In further support of our hypothesis that iron is involved, our results showed that H-DFO and SIH could abrogate cell damage induced by tBHP. H-DFO, a membrane impermeable iron chelator is exclusively taken up by cells via fluid-phase endocytosis and localized and retained within lysosomes (35, 37); consequently it can bind lysosomal iron released from the degradation of ferritins and other iron-containing proteins and block the movement of iron into other cellular compartments (36). SIH is a hydrophilic iron chelator (39). Due to its high lipophilicity, SIH can readily enter cells and tightly chelate the intracellular pool of redox-active iron. H-DFO and SIH were both found to be able to protect both induced and uninduced cells from t-BHP-mediated cell damage, implying that iron newly acquired from both extracellular sources and released from intracellular sources may be responsible for tBHP-induced cell death. Elevated HO-1 levels (data not shown) may also indicate that other heme iron-containing molecules may also release iron under the oxidative stress conditions.

To the best of our knowledge, the only pathological human condition associated with high MtFt levels are ringed sideroblasts of patients with SA (6, 51). Patients with X-linked SA have defects in erythroid-specific 5-aminolevulinic acid synthase, which leads to decreased heme synthesis in the patients' erythroblasts. The presence of iron overloaded mitochondria, which are found in such patients primarily in late erythroblasts (15), can be explained by the fact that iron is specifically targeted toward erythroid mitochondria (38, 49) and cannot be efficiently used for heme synthesis because of inhibited protoporphyrin IX formation. On the other hand, there is little evidence for inhibited protoporphyrin formation in patients with refractory anemia with ringed sideroblasts and these patients have iron overloaded mitochondria already present in early erythroblasts (15), in which the rate of heme synthesis is relatively low. Importantly, high MtFt expression in erythroblasts of such patients occurs at a very early stage of erythroid differentiation (51). Refractory anemia with ringed sideroblasts is a subcategory of myelodysplastic syndrome, which is characterized by genomic instability of hematopoietic cells and their premature apoptosis (18, 48). Hence, it is tempting to speculate that erythroid progenitors of patients with refractory anemia with ringed sideroblasts exhibiting anomalous induction of MtFt would be expected to shift a high proportion of excess cellular iron into their mitochondria (31) and render them prone to apoptosis.

Iron supplementation is widely recommended on the basis of high anemia prevalence, especially for children and pregnant women. Benefits of iron supplementation are primarily anemia prevention and correction. However, there are also concerns of potential risks of iron supplementation due to lack of elimination mechanism of iron from the body and its potential catalytic role in ROS formation (12). Despite no clear clinical manifestations of excess body iron due to dietary iron absorption in human in absence of genetic abnormalities, such as hemochromatosis, there are evidences of ROS generation associated with iron supplementation. For example, hydroxyl radical generation in chronic iron-loaded rats has been directly observed (19) and iron-deficient intestine is more susceptible to oxidative damage during iron supplementation (50). Our results may suggest that when intracellular iron storage protein levels are low, increased extracellular iron may be harmful for cells under oxidative stress conditions. There are many human diseases, such as hereditary or secondary hemochromatosis, associated with oxidative stress (12). The current study may have implications regarding systemic iron supplements, since excess iron may mediate cellular dysfunction which may lead to cell death and subsequent tissue damage (19).

In summary, we observed that MtFt expression sensitized cells to tBHP-induced oxidative stress and provided evidence that this occurs via an iron-mediated mechanism. Moreover, we demonstrated that hydrophilic and lysosomal iron chelators confer protection against tBHP induced damage and that the degree of protection was more prominent in MtFt-expressing cells. Our data also suggest that anomalous induction of MtFt may play a role in some pathological conditions such as refractory anemia with ringed sideroblasts.

Acknowledgments

This work was supported by grants from the Canadian Institutes of Health Research, Ottawa (PP) and the National Natural Science Foundation of China (30370361) and Major Project (10490181) (BZ) and 973 Grant (2006CB500700). GN gratefully acknowledges the support of Chinese Academy of Sciences, Hundred Elites Program and K. C. Wong Education Foundation, Hong Kong. We thank Brandi Wasyluk and Marc Mikhael for their generous help. H-DFO was a generous gift from Biomedical Frontiers Inc. (Minneapolis, MN).

Abbreviations

DCF-DA, 2′, 7′-dichlorofluorescin diacetate; GSH, reduced form of glutathione; GSSG, oxidized form of glutathione; H-DFO, high molecular weight desferrioxamine; MtFt, mitochondrial ferritin; PI, propidium iodide; ROS, reactive oxygen species; SA, sideroblastic anemia; tBHP, tert-butyl hydroperoxide; tet, tetracycline; TfR, transferrin receptor.

Author Disclosure Statement

No competing financial interests exist.

References

1. Arosio P and Levi S. Ferritin, iron homeostasis, and oxidative damage. *Free Radic Biol Med* 33: 457–463, 2002.
2. Balla G, Jacob HS, Balla J, Rosenberg M, Nath K, Apple F, Eaton JW, and Vercellotti GM. Ferritin: A cytoprotective antioxidant strategem of endothelium. *J Biol Chem* 267: 18148–18153, 1992.

3. Bottomley SS. Congenital sideroblastic anemias. *Curr Hematol Rep* 5: 41–49, 2006.
4. Caltagirone A, Weiss G, and Pantopoulos K. Modulation of cellular iron metabolism by hydrogen peroxide. Effects of H_2O_2 on the expression and function of iron-responsive element-containing mRNAs in B6 fibroblasts. *J Biol Chem* 276: 19738–19745, 2001.
5. Campanella A, Isaya G, O'Neill HA, Santambrogio P, Cozzi A, Arosio P, and Levi S. The expression of human mitochondrial ferritin rescues respiratory function in frataxin-deficient yeast. *Hum Mol Genet* 13: 2279–2288, 2004.
6. Cazzola M, Invernizzi R, Bergamaschi G, Levi S, Corsi B, Travaglino E, Rolandi V, Biasiotto G, Drysdale J, and Arosio P. Mitochondrial ferritin expression in erythroid cells from patients with sideroblastic anemia. *Blood* 101: 1996–2000, 2003.
7. Corsi B, Cozzi A, Arosio P, Drysdale J, Santambrogio P, Campanella A, Biasiotto G, Albertini A, and Levi S. Human mitochondrial ferritin expressed in HeLa cells incorporates iron and affects cellular iron metabolism. *J Biol Chem* 277: 22430–22437, 2002.
8. Cozzi A, Corsi B, Levi S, Santambrogio P, Albertini A, and Arosio P. Overexpression of wild type and mutated human ferritin H-chain in HeLa cells: *In vivo* role of ferritin ferroxidase activity. *J Biol Chem* 275: 25122–25129, 2000.
9. Dalton TP, Chen Y, Schneider SN, Nebert DW, and Shertzer HG. Genetically altered mice to evaluate glutathione homeostasis in health and disease. *Free Radic Biol Med* 37: 1511–1526, 2004.
10. De D, I, McVey WD, and Kaplan J. Regulation of iron acquisition and storage: Consequences for iron-linked disorders. *Nat Rev Mol Cell Biol* 9: 72–81, 2008.
11. Drysdale J, Arosio P, Invernizzi R, Cazzola M, Volz A, Corsi B, Biasiotto G, and Levi S. Mitochondrial ferritin: a new player in iron metabolism. *Blood Cells Mol Dis* 29: 376–383, 2002.
12. Eaton JW and Qian M. Molecular bases of cellular iron toxicity. *Free Radic Biol Med* 32: 833–840, 2002.
13. Epsztejn S, Glickstein H, Picard V, Slotki IN, Breuer W, Beaumont C, and Cabantchik ZI. H-ferritin subunit overexpression in erythroid cells reduces the oxidative stress response and induces multidrug resistance properties. *Blood* 94: 3593–3603, 1999.
14. Fleming MD. The genetics of inherited sideroblastic anemias. *Semin Hematol* 39: 270–281, 2002.
15. Hall R and Losowsky MS. The distribution of erythroblast iron in sideroblastic anaemias. *Br J Haematol* 12: 334–340, 1966.
16. Hallaway PE, Eaton JW, Panter SS, and Hedlund BE. Modulation of deferoxamine toxicity and clearance by covalent attachment to biocompatible polymers. *Proc Natl Acad Sci USA* 86: 10108–10112, 1989.
17. Harrison PM and Arosio P. The ferritins: Molecular properties, iron storage function and cellular regulation. *Biochim Biophys Acta* 1275: 161–203, 1996.
18. Hofmann WK and Koeffler HP. Myelodysplastic syndrome. *Annu Rev Med* 56: 1–16, 2005.
19. Kadiiska MB, Burkitt MJ, Xiang QH, and Mason RP. Iron supplementation generates hydroxyl radical *in vivo*. An ESR spin-trapping investigation. *J Clin Invest* 96:1653–1657, 1995.
20. Kakhlon O, Gruenbaum Y, and Cabantchik ZI. Repression of ferritin expression increases the labile iron pool, oxidative stress, and short-term growth of human erythroleukemia cells. *Blood* 97: 2863–2871, 2001.
21. Kotamraju S, Tampo Y, Keszler A, Chitambar CR, Joseph J, Haas AL, and Kalyanaraman B. Nitric oxide inhibits H2O2-induced transferrin receptor-dependent apoptosis in endothelial cells: Role of ubiquitin-proteasome pathway. *Proc Natl Acad Sci USA* 100: 10653–10658, 2003.
22. Kurz T, Leake A, Von Zglinicki T, and Brunk UT. Relocalized redox-active lysosomal iron is an important mediator of oxidative-stress-induced DNA damage. *Biochem J* 378: 1039–1045, 2004.
23. Langlois dB, Santambrogio P, Granier T, Gallois B, Chevalier JM, Precigoux G, Levi S, and Arosio P. Crystal structure and biochemical properties of the human mitochondrial ferritin and its mutant Ser144Ala. *J Mol Biol* 340: 277–293, 2004.
24. Levi S, Corsi B, Bosisio M, Invernizzi R, Volz A, Sanford D, Arosio P, and Drysdale J. A human mitochondrial ferritin encoded by an intronless gene. *J Biol Chem* 276: 24437–24440, 2001.
25. Lill R and Muhlenhoff U. Iron–sulfur protein biogenesis in eukaryotes: Components and mechanisms. *Annu Rev Cell Dev Biol* 22: 457–486, 2006.
26. May A and Fitzsimons E. Sideroblastic anaemia. *Baillieres Clin Haematol* 7: 851–879, 1994.
27. Mirjolet JF, Barberi–Heyob M, Didelot C, Peyrat JP, Abecassis J, Millon R, and Merlin JL. Bcl-2/Bax protein ratio predicts 5-fluorouracil sensitivity independently of p53 status. *Br J Cancer* 83: 1380–1386, 2000.
28. Missirlis F, Holmberg S, Georgieva T, Dunkov BC, Rouault TA, and Law JH. Characterization of mitochondrial ferritin in *Drosophila*. *Proc Natl Acad Sci USA* 103: 5893–5898, 2006.
29. Napier I, Ponka P, and Richardson DR. Iron trafficking in the mitochondrion: Novel pathways revealed by disease. *Blood* 105: 1867–1874, 2005.
30. Nie G, Chen G, Sheftel AD, Pantopoulos K, and Ponka P. *In vivo* tumor growth is inhibited by cytosolic iron deprivation caused by the expression of mitochondrial ferritin. *Blood* 108: 2428–2434, 2006.
31. Nie G, Sheftel AD, Kim SF, and Ponka P. Overexpression of mitochondrial ferritin causes cytosolic iron depletion and changes cellular iron homeostasis. *Blood* 105: 2161–2167, 2005.
32. Orino K, Tsuji Y, Torti FM, and Torti SV. Adenovirus E1A blocks oxidant-dependent ferritin induction and sensitizes cells to pro-oxidant cytotoxicity. *FEBS Lett* 461: 334–338, 1999.
33. Pandolfo M. Iron and Friedreich ataxia. *J Neural Transm Suppl* 143–146, 2006.
34. Pantopoulos K and Hentze MW. Activation of iron regulatory protein-1 by oxidative stress *in vitro*. *Proc Natl Acad Sci USA* 95: 10559–10563, 1998.
35. Persson HL, Kurz T, Eaton JW, and Brunk UT. Radiation-induced cell death: importance of lysosomal destabilization. *Biochem J* 389: 877–884, 2005.
36. Persson HL and Richardson DR. Iron-binding drugs targeted to lysosomes: A potential strategy to treat inflammatory lung disorders. *Expert Opin Investig Drugs* 14: 997–1008, 2005.
37. Persson HL, Yu Z, Tirosh O, Eaton JW, and Brunk UT. Prevention of oxidant-induced cell death by lysosomotropic iron chelators. *Free Radic Biol Med* 34: 1295–1305, 2003.
38. Ponka P. Tissue-specific regulation of iron metabolism and heme synthesis: Distinct control mechanisms in erythroid cells. *Blood* 89: 1–25, 1997.
39. Ponka P, Borova J, Neuwirt J, Fuchs O, and Necas E. A study of intracellular iron metabolism using pyridoxal isonicotinoyl hydrazone and other synthetic chelating agents. *Biochim Biophys Acta* 586: 278–297, 1979.
40. Ponka P and Schulman HM. Acquisition of iron from transferrin regulates reticulocyte heme synthesis. *J Biol Chem* 260: 14717–14721, 1985.

41. Radisky DC and Kaplan J. Iron in cytosolic ferritin can be recycled through lysosomal degradation in human fibroblasts. *Biochem J* 336: 201–205, 1998.
42. Raisova M, Hossini AM, Eberle J, Riebeling C, Wieder T, Sturm I, Daniel PT, Orfanos CE, and Geilen CC. The Bax/Bcl-2 ratio determines the susceptibility of human melanoma cells to CD95/Fas-mediated apoptosis. *J Invest Dermatol* 117: 333–340, 2001.
43. Richardson DR and Ponka P. The molecular mechanisms of the metabolism and transport of iron in normal and neoplastic cells. *Biochim Biophys Acta* 1331: 1–40, 1997.
44. Roberg K, Johansson U and Ollinger K. Lysosomal release of cathepsin D precedes relocation of cytochrome c and loss of mitochondrial transmembrane potential during apoptosis induced by oxidative stress. *Free Radic Biol Med* 27: 1228–1237, 1999.
45. Roberg K and Ollinger K. Oxidative stress causes relocation of the lysosomal enzyme cathepsin D with ensuing apoptosis in neonatal rat cardiomyocytes. *Am J Pathol* 152: 1151–1156, 1998.
46. Rouault TA and Tong WH. Iron–sulphur cluster biogenesis and mitochondrial iron homeostasis. *Nat Rev Mol Cell Biol* 6: 345–351, 2005.
47. Santambrogio P, Biasiotto G, Sanvito F, Olivieri S, Arosio P, and Levi S. Mitochondrial ferritin expression in adult mouse tissues. *J Histochem Cytochem* 55: 1129–1137, 2007.
48. Sekeres MA. The myelodysplastic syndromes. *Expert Opin Biol Ther* 7: 369–377, 2007.
49. Sheftel AD, Zhang AS, Brown C, Shirihai OS, and Ponka P. Direct interorganellar transfer of iron from endosome to mitochondrion. *Blood* 110: 125–132, 2007.
50. Srigiridhar K and Nair KM. Iron-deficient intestine is more susceptible to peroxidative damage during iron supplementation in rats. *Free Radic Biol Med* 25: 660–665, 1998.
51. Tehranchi R, Invernizzi R, Grandien A, Zhivotovsky B, Fadeel B, Forsblom AM, Travaglino E, Samuelsson J, Hast R, Nilsson L, Cazzola M, Wibom R, and Hellstrom–Lindberg E. Aberrant mitochondrial iron distribution and maturation arrest characterize early erythroid precursors in low-risk myelodysplastic syndromes. *Blood* 106: 247–253, 2005.
52. Theil EC, Matzapetakis M, and Liu X. Ferritins: Iron/oxygen biominerals in protein nanocages. *J Biol Inorg Chem* 11: 803–810, 2006.
53. Torti FM and Torti SV. Regulation of ferritin genes and protein. *Blood* 99: 3505–3516, 2002.
54. Tsuji Y, Ayaki H, Whitman SP, Morrow CS, Torti SV, and Torti FM. Coordinate transcriptional and translational regulation of ferritin in response to oxidative stress. *Mol Cell Biol* 20: 5818–5827, 2000.
55. Vessey DA, Lee KH, Blacker KL. Characterization of the oxidative stress initiated in cultured human keratinocytes by treatment with peroxides. *J Invest Dermatol* 99: 859–863, 1992.
56. Zanella I, Derosas M, Corrado M, Cocco E, Cavadini P, Biasiotto G, Poli M, Verardi R, and Arosio P. The effects of frataxin silencing in HeLa cells are rescued by the expression of human mitochondrial ferritin. *Biochim Biophys Acta* 1782: 90–98, 2008.
57. Zhang Y and Zhao B. Green tea polyphenols enhance sodium nitroprusside-induced neurotoxicity in human neuroblastoma SH-SY5Y cells. *J Neurochem* 86: 1189–1200, 2003.

Address correspondence to:
Dr. Prem Ponka
Lady Davis Institute for Medical Research
Sir Mortimer B. Davis Jewish General Hospital
McGill University
3755 Cote Ste-Catherine Road
Montreal, Québec
H3T 1E2, Canada

E-mail: prem.ponka@mcgill.ca

and

Dr. Baolu Zhao
Institute of Biophysics
The Chinese Academy of Sciences
15 Datun Road
Chaoyang District, Beijing
100101, PR China

E-mail: zhaobl@sun5.ibp.ac.cn

Date of first submission to ARS Central, September 22, 2008; date of final revised submission, March 4, 2009; date of acceptance, March 7, 2009.

This article has been cited by:

1. Yinghui Zhang , Marc Mikhael , Dongxue Xu , Yiye Li , Shan Soe-Lin , Bo Ning , Wei Li , Guangjun Nie , Yuliang Zhao , Prem Ponka . 2010. Lysosomal Proteolysis Is the Primary Degradation Pathway for Cytosolic Ferritin and Cytosolic Ferritin Degradation Is Necessary for Iron Exit. *Antioxidants & Redox Signaling* **13**:7, 999-1009. [Abstract] [Full Text HTML] [Full Text PDF] [Full Text PDF with Links]
2. Zhen-Hua Shi , Guangjun Nie , Xiang-Lin Duan , Tracey Rouault , Wen-Shuang Wu , Bo Ning , Nan Zhang , Yan-Zhong Chang , Bao-Lu Zhao . 2010. Neuroprotective Mechanism of Mitochondrial Ferritin on 6-Hydroxydopamine–Induced Dopaminergic Cell Damage: Implication for Neuroprotection in Parkinson's Disease. *Antioxidants & Redox Signaling* **13**:6, 783-796. [Abstract] [Full Text HTML] [Full Text PDF] [Full Text PDF with Links]
3. Paolo Arosio, Sonia Levi. 2010. Cytosolic and mitochondrial ferritins in the regulation of cellular iron homeostasis and oxidative damage. *Biochimica et Biophysica Acta (BBA) - General Subjects* **1800**:8, 783-792. [CrossRef]
4. Siddhartha Mondragón-Rodríguez, Gustavo Basurto-Islas, Hyoung-gon Lee, George Perry, Xiongwei Zhu, Rudy J Castellani, Mark A Smith. 2010. Causes versus effects: the increasing complexities of Alzheimer’s disease pathogenesis. *Expert Review of Neurotherapeutics* **10**:5, 683-691. [CrossRef]